

Progress towards tubes with regular nanopatterned inner surfaces

K. Seunarine, M. Tormen, N. Gadegaard, M. Riehle, C. D. Wilkinson et al.

Citation: *J. Vac. Sci. Technol. B* **24**, 3258 (2006); doi: 10.1116/1.2357970

View online: <http://dx.doi.org/10.1116/1.2357970>

View Table of Contents: <http://avspublications.org/resource/1/JVTBD9/v24/i6>

Published by the AVS: Science & Technology of Materials, Interfaces, and Processing

Related Articles

Enzyme adsorption on polymer-based confined bioinspired biosensing surface

J. Vac. Sci. Technol. A **30**, 050607 (2012)

Micro- and nanostructured poly[oligo(ethylene glycol)methacrylate] brushes grown from photopatterned halogen initiators by atom transfer radical polymerization

Biointerphases **6**, 8 (2011)

Photolithographic synthesis of high-density DNA probe arrays: Challenges and opportunities

J. Vac. Sci. Technol. B **25**, 2537 (2007)

Nanoscale eluting coatings based on alginate/chitosan hydrogels

Biointerphases **2**, 95 (2007)

Nanoimprint fabrication of polymer cell substrates with combined microscale and nanoscale topography

J. Vac. Sci. Technol. B **25**, L31 (2007)

Additional information on *J. Vac. Sci. Technol. B*

Journal Homepage: <http://avspublications.org/jvstb>

Journal Information: http://avspublications.org/jvstb/about/about_the_journal

Top downloads: http://avspublications.org/jvstb/top_20_most_downloaded

Information for Authors: http://avspublications.org/jvstb/authors/information_for_contributors

ADVERTISEMENT

 <p>AVS 59th International Symposium & Exhibition October 28–November 2, 2012 • Tampa, Florida</p> <p>212-248-0200 avsnyc@avs.org www.avs.org</p>		<p>DIVISION/GROUP PROGRAMS:</p> <ul style="list-style-type: none"> • Advanced Surface Engineering • Applied Surface Science • Biomaterial Interfaces • Electronic Materials & Processing • Magnetic Interfaces & Nanostructures • Manufacturing Science & Technology • MEMS & NEMS • Nanometer-Scale Science & Technology • Plasma Science & Technology • Surface Science • Thin Film • Vacuum Technology 	<p>FOCUS TOPICS:</p> <ul style="list-style-type: none"> • Actinides & Rare Earths • Biofilms & Biofouling: Marine, Medical, Energy • Biointerphases • Electron Transport at the Nanoscale • Energy Frontiers • Exhibitor Technology Spotlight • Graphene & Related Materials • Helium Ion Microscopy • <i>InSitu</i> Microscopy & Spectroscopy • Nanomanufacturing • Oxide Heterostructures-Interface Form & Function • Scanning Probe Microscopy • Spectroscopic Ellipsometry • Transparent Conductors & Printable Electronics • Tribology
--	--	--	---

Progress towards tubes with regular nanopatterned inner surfaces

K. Seunarine^{a)}

Centre for Cell Engineering, Glasgow University, Glasgow G12 8QQ, Great Britain

M. Tormen

TASC Laboratory of the Istituto Nazionale della Fisica della Materia, S.S. 14 km. 163.5, I-34012 Basovizza-Trieste, Italy

N. Gadegaard, M. Riehle, and C. D. W. Wilkinson

Centre for Cell Engineering, Glasgow University, Glasgow G12 8QQ, Great Britain

L. Businaro and F. Romanato

TASC Laboratory of the Istituto Nazionale della Fisica della Materia, S.S. 14 km. 163.5, I-34012 Basovizza-Trieste, Italy

(Received 31 May 2006; accepted 28 August 2006; published 4 December 2006)

The repair of vascular tubing is an important task in tissue engineering. The behavior of cells is strongly influenced by the topology of the surfaces, on both a micrometric and a nanometric scale, in their vicinity. Thus the authors wish to make tubes that are patterned on the inner surface. One way to do this is to use the good depth of focus capabilities of x-ray exposure to print an array of dots, 200 nm diameter and 400 nm pitch, onto a curved surface coated in resist. A die made from this structure allows nanoembossing into a biodegradable polymer. A closed vessel can then be made by adding a lid, that also has a similar nanopatterned surface. Details of the accuracy of transfer are given. It is concluded that x-ray printing is a suitable approach for the formation of internally patterned tubing. © 2006 American Vacuum Society. [DOI: 10.1116/1.2357970]

I. INTRODUCTION

Tubular structures are of great importance in the functioning of the body. They provide a means of fluid transport to supply organs and tissues with the nutrients they need as well as remove waste products. They can be damaged and prostheses for the repair of vascular tissue are needed. The innermost layer of cells in the vascular system is of vital importance; this layer of cells must both seal the fluid in the tube from the surrounding tissue and prevent adhesion of any cells in the fluid to the walls (for example, prevent the activation of platelets in arterial blood). Patterning with regular patterns of topographic features on a nanometric scale has been shown to have a profound effect on the adhesion, proliferation, gene expression, and possibly even the differentiation of cells.^{1,2}

We know from earlier work that tendon and fibroblast cells have low adhesion properties on regular arrays of nanopattern pits and pillars (100–200 nm diameter on a 300 nm center-to-center spacing).^{3,4}

The micrograph in Fig. 1 shows a polycaprolactone substrate that has been embossed with a stamp made up of several arrays of nanopits; each array consists of pits of a different diameter. Human telomerase reverse transcriptase (hTERT) cells are seeded onto the substrate and cultured for 72 h before being fixed and stained. [hTERT cells are a human fibroblast cell line transfected with the hTERT vector which allows for theoretically infinite replication. Fibroblasts are ubiquitous cells that are present in connective tissue and also found in the wound healing (implant) environment.] The

light areas of the substrate represent areas with a sparse population of cells; it is clear that the nano-topography affects the adhesion.

A previous attempt to make fully functional blood vessels was reported by Goodman *et al.* They used a 1:1 mixture of methylmethacrylate monomer and a proprietary low molecular weight methacrylate prepolymer to cast inverse replicas of 1–4 mm internal diameter mammalian arteries and veins. Following removal of the arterial tissue a positive replica, onto which cells were seeded to form a new blood vessel, was made by solution casting polyurethane upon the surface of the inverse replica. The inverse replica was dissolved in acetone to expose the positive replica.⁵

It will be useful to make tubing of biodegradable polymeric material with biodegradable polymeric material with a nanopatterned inner surface. The rolling up of a nanopatterned flat sheet inevitably leaves an incorrectly patterned area in the region of the join. In this region the prosthesis would be fatally flawed.

We have previously reported on a technique for forming nanostructures on nonflat surfaces, but this method involved writing on an initially flat surface and then deforming the substrate to produce features on surfaces with large curvature—this technique is in the early stages of development.⁶

Gadegaard *et al.* have also patterned the interior of tubes using a method based on the phenomenon of phase separation of incompatible polymer blends.⁷ Previous experiments have demonstrated that the particular topography formed by polymer demixing of flat surfaces had a pronounced effect on cell adhesion and proliferation.^{8,9} However, the materials

^{a)}Electronic mail: ks@elec.gla.ac.uk

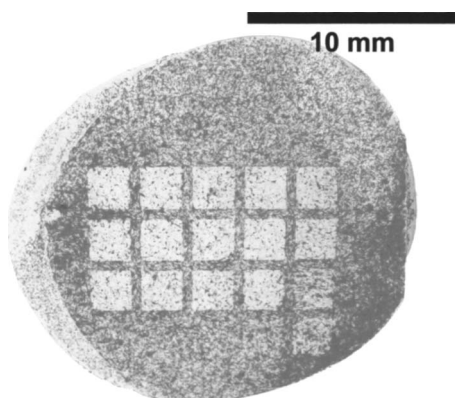


FIG. 1. hTERT cells after 72 h on a nanopatterned PCL substrate. The nanopatterned areas appear as light and so have few cells. These square areas consist of arrays of nanopits of different diameters. The pit diameters increase from the square at the top left to square at the bottom left in a raster fashion. Micrograph courtesy of E. Martines.

used for forming the nanotopography as well as the tube would prevent this system from being used in the body.

Three-dimensional surfaces have been produced by e-beam lithography using dose modulation.^{10,11} While this produces excellent devices for diffractive optics, very slight variations in dosage at field boundaries produce shallow linear features. This causes only minor scattering in optical applications, but are features onto which cells adhere and align.¹²

The depth of focus in electron beam lithography depends on the convergence angle of the beam. For example, in our Leica Microsystems EBPG 5 beam writer, a spot of diameter of 80 nm in the focal plane increases to 170 nm at a defocus of 15 μm (aperture-stage separation of 40 mm, aperture diameter of 400 μm). This variation in spot size is too great for the present application. X-ray lithography has more depth of focus.

We describe a method that uses proximity x-ray lithography to print nanopatterns on curved surfaces (Fig. 2). A quartz grating is coated with polymethylmethacrylate (PMMA) and a nanopattern transferred by x-ray lithography. The PMMA is developed in isopropyl alcohol¹³ IPA before being coated with a conductive base layer and electroplated to make a nickel shim that can be used to emboss into sheets of biodegradable polymer.

A nanopatterned lid is made by hot embossing and the two embossed structures are bonded together to form an enclosed half-pipe with internal nanopatterning.

II. EXPERIMENT

A. State of the art in x-ray printing

The printing of very fine features using x-rays onto a curved substrate coated in resist is limited by Fresnel diffraction of the beam. The realized size of the developed feature in resist depends on the (varying) gap between substrate and mask, the absorption of the patterned regions of the mask, and the exposure and development conditions.

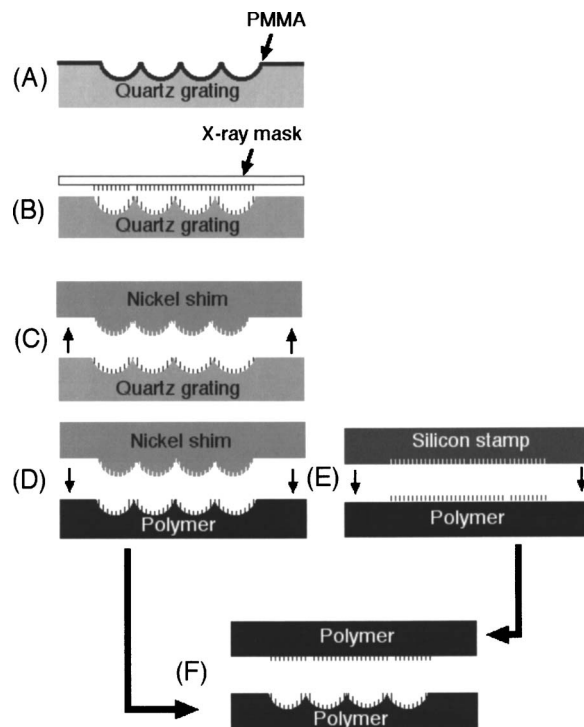


FIG. 2. Schematic illustration of the fabrication procedure. (A) Quartz grating is coated with PMMA. (B) Nanostructure is formed in the PMMA by x-ray lithography. (C) After development a nickel shim is made from the 3D nanopatterned structure. (D) Nickel shim is used to prepare many replicas in a biodegradable polymer. (E) Micropatterned lid is embossed. (F) Complete tubular structure is made by bonding the 3D substrate with the lid.

In a paper on the use of x-rays in the decananometric region for silicon very large scale integration, Toyota and Washio¹⁴ show, from simulation and an analysis of worker's results, that under the best conditions, the maximum gap g is of the order

$$g = \alpha w^2 / \lambda,$$

where w is the half-pitch, λ is the wavelength, and α is around 2.6.¹⁴ Using this with a half-pitch of 200 nm and a wavelength corresponding to 1.6 keV gives a maximum gap of around 130 μm .

B. Micrometric quartz grating fabrication

The initial step is to make a quartz substrate with a half-pipe profile (80 μm period and 10.05 μm depth). An 80 nm thick chrome mask layer is sputter coated on the quartz substrate. An overlying layer of photoresist is patterned by photolithography and the pattern, consisting of narrow openings on an 80 μm period, is transferred to the chromium layer by wet etching in an aqueous solution of ammonium cerium IV nitrate and acetic acid. The quartz is etched isotropically in aqueous HF (48 wt %) at room temperature, at an etching rate s of 1100 nm/min, for a time t . The resulting hemicylindrical holes have a radius of st (and the same maximum depth), Fig. 3. The chromium mask is removed and the substrate etched again in aqueous HF for a time t_1 . During this additional etching time, the radius of curvature of the open-

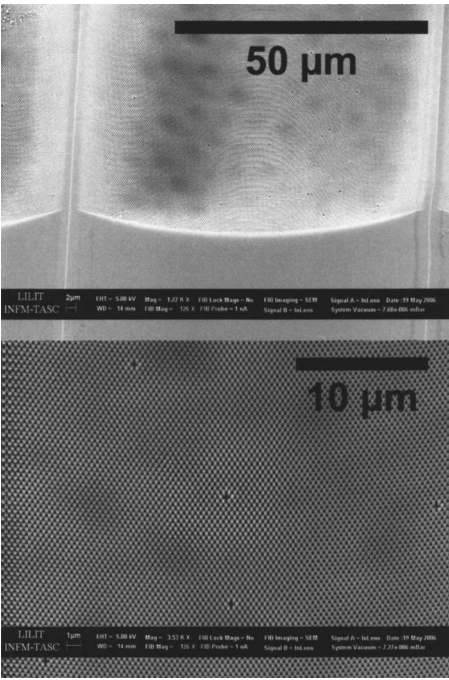


FIG. 6. Scanning electron micrograph of the nanopatterned resist on a quartz grating: Low magnification (top); high magnification (bottom).

The pillars at the top of the grating structure were ~ 213 nm in diameter, while the pillars at the bottom of the grating were ~ 178 nm in diameter, Fig. 7.

Fresnel diffraction reveals itself in a variety of ways. The hole in the center of the pillars is due to this cause, as is the slightly hexagonal shape of the pillars. This distortion from a circular shape is more pronounced at the top of the structure

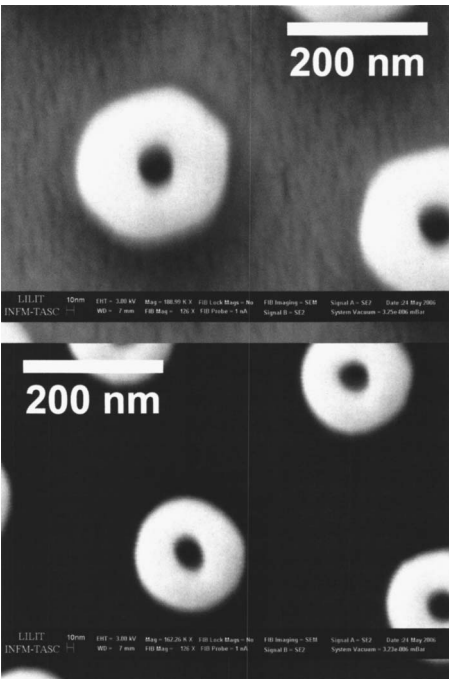


FIG. 7. Pillars at the top of the grating (top) are ~ 213 nm in diameter while the pillars at the bottom of the structure are ~ 178 nm in diameter.

TABLE I. Lid stamp is etched in an ICP. The gases are unswitched to avoid scalloping.

Gases	C_4F_8 , 120 SCCM; SF_6 , 40 SCCM (no switching)
Pressure	10 mT
Power	525 W coil, 18 W platen
Etch rate	100 nm/min

than at the bottom. It is believed that optimization of the spectrum should be able to reduce the unwanted peak in intensity in the shadow zone.

D. Nanopatterned lid fabrication

A silicon stamp is made for embossing the lid. A silicon substrate is coated with ZEP520A:anisole (40:60) at the rate of 5 krpm for 60 s, then baked in an oven for 60 min at $180^\circ C$. Following e-beam writing (Leica EBPG 5) the resist is developed in *o*-xylene at $24^\circ C$ for 60 s. The silicon is etched in an inductively coupled plasma (ICP) from Oxford Plasma Technology for 1 min, Table I. Following plasma etching the remaining resist is removed by a 5 min sulfuric acid:hydrogen peroxide (7:1) etch. This cleaning step also oxidizes the silicon prior to an antiadhesion layer coating step. The silicon stamp is immersed in a mixture of $29 \mu l$ of perfluorosilane ($C_8H_4Cl_3F_{13}Si$), from Gelest, and 100 ml of heptane for approximately 1 h. The stamp is then removed from the perfluorosilane/heptane mixture and cleaned by gentle rinsing in heptane, acetone, ethanol, and finally ethanol:water (1:1), Fig. 8.

The stamp is used to emboss a sheet of polycaprolactone (PCL) by melt embossing in an optical press.¹⁸

III. DISCUSSION

X-ray lithography has been used to transfer nanopillar patterns into PMMA resist on an isotropically etched grating structure that has a $10 \mu m$ variation in height. The critical stages of substrate formation, mask formation, transfer of pattern onto the curved surface, and embossing on this scale have been successfully demonstrated. The next step is to increase the variation in height towards the ideal value for the present purpose of studying the behavior of cells in vas-

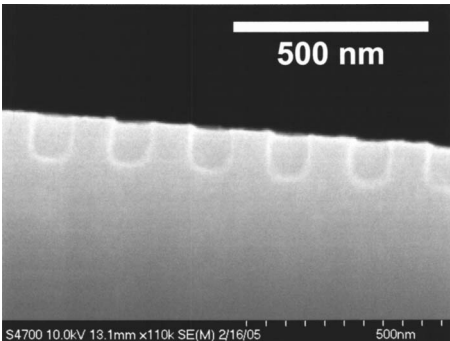


FIG. 8. Nanopits are fabricated on silicon stamp by e-beam lithography and dry etching.

cular tubes of about 50 μm . The possibility of bonding two half-pipes together, giving twice the height, rather than putting a lid on a single half-pipe is unfortunately not open to us, as the alignment of the two halves after heat bonding would have to be perfect to 100 nm if a linear flat feature of the type cells delight to inhabit is to be avoided.

It is clear that x-ray lithography is a suitable method for forming the three-dimensional (3D) structures required in cell engineering.

ACKNOWLEDGMENTS

The partial support by the EC-funded project NaPa (Contract No. NMP4-CT-2003-500120) is gratefully acknowledged. One of the authors (N.G.) is supported through a Royal Society of Edinburgh fellowship. The authors also wish to thank S. Thoms for his useful discussions.

¹A. S. G. Curtis and C. D. W. Wilkinson, *Trends Biotechnol.* **19**, 97 (2001).

²M. J. Dalby, S. J. Yarwood, M. O. Riehle, H. J. H. Johnstone, S. Affrossman, and A. S. G. Curtis, *Exp. Cell Res.* **276**, 1 (2002).

³J. O. Gallagher, K. F. McGhee, C. D. W. Wilkinson, and M. O. Riehle, *IEEE Trans. Nanobiosci.* **1**, 24 (2003).

⁴M. J. Dalby, N. Gadegaard, M. O. Riehle, C. D. W. Wilkinson, and A. S.

G. Curtis, *Int. J. Biochem. Cell Biol.* **36** (2005).

⁵S. L. Goodman, P. A. Sims, and R. M. Albrecht, *Biomaterials* **17**, 2087 (1996).

⁶N. Gadegaard, E. Martinez, M. O. Riehle, K. Seunarine, and C. D. W. Wilkinson, *Microelectron. Eng.* **83**, 1577 (2006).

⁷N. Gadegaard, M. J. Dalby, M. O. Riehle, A. S. G. Curtis, and S. Affrossman, *Adv. Mater. (Weinheim, Ger.)* **16**, 1857 (2004).

⁸M. J. Dalby, M. O. Riehle, H. Johnstone, S. Affrossman, and A. S. G. Curtis, *Biomaterials* **23**, 2945 (2002).

⁹M. J. Dalby, M. O. Riehle, H. J. H. Johnstone, S. Affrossman, and A. S. G. Curtis, *Tissue Eng.* **8**, 1099 (2002).

¹⁰V. V. Aristov, S. V. Dubonos, R. Y. Dyachenko, B. N. Gaifullin, V. N. Matveev, H. Raith, A. A. Svinstov, and S. I. Zaitsev, *J. Vac. Sci. Technol. B* **13**, 2526 (1995).

¹¹D. R. S. Cumming, I. I. Khandaker, S. Thoms, and B. G. Casey, *J. Vac. Sci. Technol. B* **15**, 2859 (1997).

¹²B. Wójciak-Stothard, A. Curtis, W. Monaghan, K. Macdonald, and C. Wilkinson, *Exp. Cell Res.* **223**, 426 (1996).

¹³O. Dial, C. C. Cheng, and A. Scherer, *J. Vac. Sci. Technol. B* **16**, 3887 (1998).

¹⁴E. Toyota and M. Washio, *J. Vac. Sci. Technol. B* **20**, 2979 (2002).

¹⁵M. Tormen, A. Carpentiero, L. Vaccari, M. Altissimo, D. Cojoc, and E. Di Fabrizio, *J. Vac. Sci. Technol. B* **23**, 2920 (2005).

¹⁶F. Romanato, E. Di Fabrizio, L. Vaccari, M. Altissimo, D. Cojoc, L. Businaro, and S. Cabrini, *Microelectron. Eng.* **57/58**, 101 (2001).

¹⁷F. Romanato, M. Tormen, L. Businaro, L. Vaccari, T. Stomeo, A. Passaseo, and E. Di Fabrizio, *Microelectron. Eng.* **73–74**, 870 (2004).

¹⁸K. Seunarine, N. Gadegaard, M. O. Riehle, and C. D. W. Wilkinson, *Microelectron. Eng.* **83**, 859 (2006).